# Chapter 14
# MD/FE Multiscale Modeling of Contact

**Srinivasa Babu Ramisetti, Guillaume Anciaux and Jean-Francois Molinari**

**Abstract** Limitations of single scale approaches to study the complex physics involved in friction have motivated the development of multiscale models. We review the state-of-the-art multiscale models that have been developed up to date. These have been successfully applied to a variety of physical problems, but that were limited, in most cases, to zero Kelvin studies. We illustrate some of the technical challenges involved with simulating a frictional sliding problem, which by nature generates a large amount of heat. These challenges can be overcome by a proper usage of spatial filters, which we combine to a direct finite-temperature multiscale approach coupling molecular dynamics with finite elements. The basic building block relies on the proper definition of a scale transfer operator using the least square minimization and spatial filtering. Then, the restitution force from the generalized Langevin equation is modified to perform a two-way thermal coupling between the two models. Numerical examples are shown to illustrate the proposed coupling formulation.

## 14.1 Introduction

Traditional friction experiments are particularly difficult to comprehend since they involve a wide variety of physical mechanisms that interact at several length and time scales. Amongst those mechanisms, one can list for instance long range elastic deformations, plasticity, third body interactions, lattice dynamics and heat transfer [1]. An additional difficulty comes from their interactions with surface topology. Experimental, theoretical and numerical studies have shown that surface roughness is a key determining factor for friction. Roughness being present at all length scales

S.B. Ramisetti
University of Edinburgh, Sanderson Building, Edinburgh, UK
e-mail: s.ramisetti@ed.ac.uk

G. Anciaux
Ecole Polytechnique Fédérale de Lausanne, EPFL ENAC IIC LSMS, GC A2 484
(Bâtiment GC), Station 18, 1015 Lausanne, Switzerland
e-mail: guillaume.anciaux@epfl.ch

J.F. Molinari (✉)
e-mail: jean-francois.molinari@epfl.ch



E. Gnecco and E. Meyer (eds.), *Fundamentals of Friction and Wear on the Nanoscale*,
NanoScience and Technology, DOI 10.1007/978-3-319-10560-4_14

[2], developing a fundamental understanding of how microscopic contact clusters develop under load remains an important question [3, 4].

In the last few decades, with the development of nanotechnologies and nano science, interfaces and surfaces have started to dominate over the more classical and thus better understood bulk mechanisms. This challenges our traditional design tools and in particular continuum mechanics predictions which can be shown to break down at atomistic size asperities [5]. On the other hand, novel experimental techniques such as surface force apparatus, atomic force microscopy, friction force microscopy and quartz-crystal micro-balance are now extensively used to understand the atomic origins of friction [6, 7]. These techniques provide new insights and give renewed hope that we will one day have fully predictive tools for friction.

An essential component of those tools will be numerical modeling. Simulations are not only a useful complement to experiments as they can answer several experimental unknowns, but they can be used to explore a range of conditions out of reach of experiments. While numerical contact mechanics models have traditionally relied on a macroscopic description with empirical or semi-empirical phenomenological laws (Coulomb friction law, Archard wear law), recent modeling efforts increasingly attempt to represent the accurate atomistic mechanisms and capture the statistics of contact forces at small-scale contact asperities. However, a true separation of scales does not exist in most applications, and thus it is important to couple the small scale atomic mechanisms with long-range elastic forces and a proper handling of far field boundary conditions. This can be achieved with the rapid and recent developments in multiscale methods paralleled by a continuing expansion of computational power.

This chapter will introduce the reader to current methods in multiscale modeling of contact. An emphasis will be put on sliding contact and thus we narrow the focus to methods that couple an atomistic domain (*Molecular Dynamics*, MD, to capture atomic mechanisms at contacting asperities) to a continuum domain (*Finite Elements*, FE, for an accurate representation of long range elastic forces). Incidentally, MD/FE multi-scaling is also by far the most researched and versatile approach. The chapter begins by a review of some of the main variants of FE/MD class of direct (i.e. fully coupled) multiscale model. Furthermore, the important generation of heat during sliding friction, due to plastic activity at contacting asperities, will be demonstrated to challenge most current multiscale approaches. This will show the need for novel coupling strategies capable of handling heat fluxes through interfaces between distinct scale models. The last section of this chapter will turn to the description and validation of a novel thermo-mechanical coupling method, that shows great prospect for contact simulations.

## 14.2 Modeling Techniques of Contact at Nanoscale

A large amount of numerical studies of contact problems are based on single scale approaches. Numerical techniques such as Ab-Initio [8], *Discrete Element Method* [9, 10], *Discrete Dislocation Dynamics* [11], *Finite Element Method* [12, 13] and

*Molecular Dynamics* [14–16] have been used to study contact/friction problems. Two of the most classical techniques are the *Finite Element Method* [17, 18] and the *Molecular Dynamics* [19]. A large literature has had recourse to the *Finite Element Method*, which is a computationally efficient strategy, to model contact at the asperity level [12, 20–22].

Nevertheless, recent *Finite Element Method* simulations [23] as well as atomistic studies [5] show that contact mechanics is dominated by nanoscale asperities. Continuum mechanics is unable to capture the details of force profiles at this scale. In order to represent efficiently the atomic organization and forces at contact clusters, one can resort to *Molecular Dynamics* (MD).

Classical MD is a well-established numerical approach that is used to simulate materials at nanoscales. According to the Born-Oppenheimer approximation [24, 25], atomic nuclei are treated as point particles, because they are much heavier than surrounding electrons. Therefore, classical MD consists in driving $N$ particles with the following Newtonian equation of motion:

$$m_i \frac{d^2\mathbf{r}_i}{dt^2} = \mathbf{f}_i = \sum_{\substack{j=1 \\ j\neq i}}^{N} \mathbf{F}_{ij} \tag{14.1}$$

where $m_i$ is the mass of the $i$th atom, $\mathbf{r}_i$ is its position and $\mathbf{F}_{ij}$ is the force acting on atom $i$ exerted by atom $j$. The forces perceived by particles are described by an inter-particle potential, since the force $\mathbf{f}_i$ acting on atom $i$ is equal to the gradient of the total potential energy of the system with respect to the $i$th atom position:

$$\mathbf{f}_i = -\nabla_i \Phi(\mathbf{r}_1, \mathbf{r}_2, \ldots, \mathbf{r}_N) \tag{14.2}$$

MD simulations are used to investigate nanoscale mechanisms at the origin of adhesive and friction forces [7, 14–16, 26–34]. Besides the refined mechanical description achieved by MD models, severe limitations should be noted. First, the stable timestep is usually of the order of a femtosecond which restricts long ($>100$ ns) simulation runs. Secondly, the number of atoms to materialize a small chunk of matter is restricted by the computational time [35].

The limitations of purely atomistic or purely continuum simulations, which make extremely difficult the link of simulations and experiments, have motivated research in multi-scale simulations that bridge atomistic and continuum modeling [36–44]. In these multiscale approaches, atoms can be used at contacting asperities to capture in great details contact forces, whereas *Finite Elements* (FE) are used away from the interface to accurately represent elastic forces. The main purpose of the coarse domain is to reduce significantly the number of unknowns to handle.

## 14.3 Multiscale Coupling Applied to Contact

Multiscale modeling has captured tremendous attention from different fields such as materials science, mechanics and high performance computing, which is due to its potential to perform numerical simulations that were impossible or difficult with the full atomistic simulations. Thus, during the past decades several multiscale methods have been developed to investigate material problems.

A broad classification of multiscale approaches is done in [45], which separates the field in two categories. The first contains hierarchical methods which model the different scales separately but with information flow between fine and coarse scales. While this approach avoids the technical difficulty of direct coupling between scales, which explains the reason for its wide usage, the necessary scale separation assumption can be a too strong approximation for real applications. The second category considers direct/concurrent multiscale approaches which simulate simultaneously the different length scale models. Atomistic models are used in critical regions to capture atomistic processes, while coarser models are used in regions away from complex behavior. The coherency between the atomistic and the coarser models is enforced in an interface or overlap region as illustrated on Fig. 14.1.

Concurrent approaches are relevant for sliding friction simulations where complex deformations occur at the contacting interface, while coarser scales handle long range elastic interactions and provide boundary conditions. There exist different concurrent coupling methods such as finite element atomistics method (FEAt) [50], quasicontinuum method (QC) [46, 47], coupling of length scales (CLS) [36], coupled

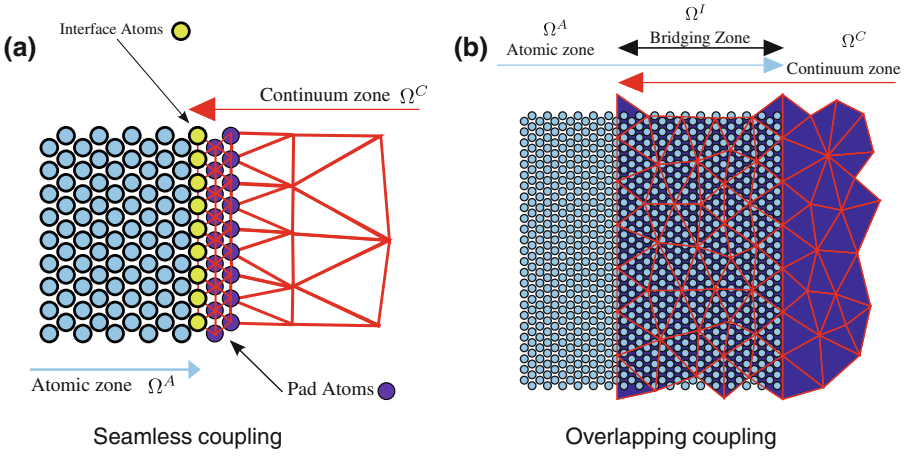


**Fig. 14.1** Illustration of coupling interfaces between molecular dynamics and finite elements. **a** Typical interface zone in a *seamless coupling* such as the *Quasi-Continuum* [46, 47], or the *Coupled Atomistic and Discrete Dislocation* [48] methods. **b** Typical bridging/overlapping zone employed in methods such as the *Bridging Domain* [49]. It should be noted that in both cases, the introduction of coarser elements leads to distinct dispersion relations and spectral decompositions

atomistic and discrete dislocation (CADD) [48], bridging scale method (BSM) [51] and bridging domain method (BDM) [49]. This list is not complete and should not be taken as the only reference. There also exists a good number of review articles, that one can refer to, which address the different multiscale methods [42, 44] and their comparison with each other [43]. Nevertheless, in the following section we will review four methods, which are now classical in the literature.

### *14.3.1 State of the Art of Multiscale Methods*

The **Quasicontinuum** (QC) method, developed by Tadmor et al. [46], was first used to investigate two-dimensional quasi-static single crystal deformation problems. In the atomic/refined region, the energy is computed using interatomic potentials. At the interface between the atoms and the FE's, the energy of the interface atoms is calculated by introducing neighboring atoms (known as pad atoms) which are deformed accordingly to interpolated FE displacement fields. In the FE region, the strain energy density $W$ is computed from the atomistic potential using the Cauchy-Born rule [46]. The total energy of the coupled system is written as:

$$E = \sum_{i \in \Omega^A} E_i + \sum_{e \in \Omega^C} w_e E_e \tag{14.3}$$

where $E_i$ is the energy of atom $i$, $E_e$ is the energy of element $e$, and $w_e$ is a weighting function to correct an energy unbalance. Indeed, the last free atoms at the interface and the first FE (pad atoms/nodes) bear an overlapped contribution to the total energy which is corrected with the weight $w_e$.

During the recent years, various improved versions of the QC method, including the treatment of multigrains and three-dimensional deformation problems, have been developed [37, 47, 52–54]. Several finite temperature extensions of the QC method exists [55–59]. For instance, the hot-QC method [56, 60] uses a temperature dependent Hamiltonian, based on the idea of the potential of mean force, to approximate the contributions of missing atoms in the continuum region.

The **Coupled Atomistic and Discrete Dislocation** (CADD) method, developed by Shilkrot et al. [48, 61], allows the direct coupling of an atomistic region with a continuum region containing dislocations. The key feature of this method is that it can pass dislocations from the atomistic region to a continuum region without confining the plastic deformation to the atomistic region in contrast to the QC method. The dislocations passed into the continuum region are represented using the discrete dislocation method [62].

As described in [48, 61], the solution to the boundary value problem is obtained by dividing it into three problems: an infinite elastic continuum with dislocations, a linear elastic continuum without any defects and a full atomistic region. The solution to the first problem is obtained by superposing the analytical elastic fields due to the network of dislocations. The stress, strain and displacement contributions from the

discrete dislocations are denoted as $\tilde{\boldsymbol{\sigma}}$, $\tilde{\boldsymbol{\varepsilon}}$, $\tilde{\mathbf{u}}$ respectively. The solution to the second problem is found by using corrective tractions $\hat{\boldsymbol{\sigma}}$ and displacements $\hat{\mathbf{u}}$. The corrective strain field is denoted by $\hat{\boldsymbol{\varepsilon}}$. And the third problem consisting of the atomistic region is solved by using interatomic potentials. The atoms near the continuum-atomistic interface are treated in the same way as in the QC method.

The total energy of the boundary value problem is expressed as:

$$E = \frac{1}{2}\int_{\Omega^C} (\tilde{\boldsymbol{\sigma}} + \hat{\boldsymbol{\sigma}}) : (\tilde{\boldsymbol{\varepsilon}} + \hat{\boldsymbol{\varepsilon}}) dV - \int_{\partial\Omega^C} \mathbf{t_0} \cdot \mathbf{u} dA + E_A - \mathbf{f}_A \cdot \mathbf{u}_A \tag{14.4}$$

where $\mathbf{t}_0$ is the prescribed traction, $\mathbf{u} = \tilde{\mathbf{u}} + \hat{\mathbf{u}}$ is the total displacement, $E_A$ is the atomistic energy, $\mathbf{f}_A$ refers to the atomic forces along the traction boundary and $\mathbf{u}_A$ refers to the atomic displacements.

The detection of the dislocations nucleated in the atomistic region and their passing to the continuum region is accomplished in two steps: (i) In 2D, a detection band of triangular elements inside region $\Omega^A$ and close to the interface is defined to monitor the Lagrangian finite strain and to allow the identification of dislocations based on their recognizable slip strains within the crystal. (ii) After the detection step, the dislocation is passed to the continuum region by adding the displacement fields associated with a dislocation dipole. This shifts the dislocation core along its slip plane from its location in the detection band to a location across the interface in the continuum region.

Currently, the approach is only validated in two-dimensional case. Extension of CADD to finite temperature simulations can be found in [63, 64], where the stadium damping method with a Langevin based thermostat is used to maintain a constant temperature of the system. However, it is not yet suitable to treat non-isothermal processes. Extension to three-dimensional systems is the subject of active research.

The **Bridging Domain method** (BDM) uses the concepts of the Arlequin approach [65–68] which can intermix energies of several continuum mechanical models and constrain consistent displacements within an overlaping zone (also termed as the bridging domain). Xiao et al. applied this strategy for coupling continuum models with molecular dynamics (MD) [49, 69].

The total Hamiltonian of the system is considered to be equal to the sum of the weighted Hamiltonians of both the atomistic and continuum models:

$$H = (1 - \alpha) E^A + \alpha E^C \tag{14.5}$$

where $E^A$ and $E^C$ are the atomic and continuum Hamiltonian contributions and where $\alpha$ is an arbitrary weighting function. The displacement continuity is enforced between the two models in the overlap region ($\Omega^I$) by constraining the degrees of freedom using the Lagrangian multiplier method. The constraints on the velocities are expressed as:

$$\mathbf{g} = \mathbf{N}\dot{\mathbf{u}} - \dot{\mathbf{d}} = 0 \tag{14.6}$$

where $\mathbf{g}$ is the vector containing per atom constraints, $\mathbf{u}$ is the FE nodal displacement, $\mathbf{d}$ is the atomic displacement and $\mathbf{N}$ is the matrix containing FE shape functions evaluated at all initial atomic positions. The governing equations for degrees of freedom inside the overlap region are formulated using the Lagrangian multiplier method. The Lagrange multipliers $\lambda$ ($L$ multipliers, with $L$ the number of coupled atoms) are obtained by solving the linear system of equations

$$\mathbf{H}\lambda = \mathbf{g}^{\star} \tag{14.7}$$

where $\mathbf{g}^{\star}$ is the constraint vector before correction and $\mathbf{H}$ is the $L \times L$ constraint matrix defined as

$$\mathbf{H} = \mathbf{N}^T \hat{\mathbf{M}}^{-1} \mathbf{N} - \hat{\mathbf{m}}^{-1} \tag{14.8}$$

where $\hat{\mathbf{M}} = \alpha \mathbf{M}$ with $\mathbf{M}$ is a coarse scale lumped mass matrix and where $\hat{\mathbf{m}} = \alpha \mathbf{m}$ with $\mathbf{m}$ is a diagonal atomic mass matrix. Finally, the discrete governing equations of the two models are expressed as follows:

$$\begin{cases} \hat{\mathbf{M}}\ddot{\mathbf{u}} = \alpha \mathbf{f}(\mathbf{u}) - \lambda \mathbf{N}^T \\ \hat{\mathbf{m}}\ddot{\mathbf{d}} = (1-\alpha)\mathbf{f}(\mathbf{d}) - \lambda \end{cases} \tag{14.9}$$

where $\mathbf{f}(\mathbf{d})$ and $\mathbf{f}(\mathbf{u})$ are the atomic and nodal forces. Details concerning the derivation of the above equations are presented in [49, 69, 70]. The arbitrary weighting is remarkably suited to dissipate spurious wave reflections [49, 70] at small temperatures ($\sim 0K$) and material problems such as fracture were successfully simulated using this method [49]. However, the application of this method to simulate finite temperature problems is difficult [71].

The **Bridging Scale method** (BSM) was developed by Wagner and Liu to concurrently couple atomistic and continuum models [51]. The idea of this method is to decompose the total displacement field $\mathbf{u}(\mathbf{x})$ into coarse and fine scales as:

$$\mathbf{u}(\mathbf{x}) = \bar{\mathbf{u}}(\mathbf{x}) + \mathbf{u}'(\mathbf{x}) \tag{14.10}$$

The coarse scale displacement field in matrix form is defined as:

$$\bar{\mathbf{u}} = \mathbf{N}\mathbf{d} \tag{14.11}$$

where $\mathbf{N}$ is the matrix containing FE shape functions evaluated at all initial atomic positions and $\mathbf{d}$ is the FE nodal displacements. The fine scale displacement field is defined as the projection of MD displacements $\mathbf{q}$ on the FE basis functions subtracted from the total solution $\mathbf{q}$ and is expressed as:

$$\mathbf{u}' = \mathbf{q} - \mathbf{P}\mathbf{q} \tag{14.12}$$

where $\mathbf{P}$ is a projection matrix defined as:

$$\mathbf{P} = \mathbf{N}\mathbf{M}^{-1}\mathbf{N}^T\mathbf{M}_A \tag{14.13}$$

Here $\mathbf{M}_A$ is a diagonal atomic mass matrix and $\mathbf{M} = \mathbf{N}^T\mathbf{M}_A\mathbf{N}$ is a coarse scale mass matrix.

The final equations of motion for the MD and FE models are derived using the Lagrangian form. More details about the derivation of these equations can be found in [72]. The key equations are:

$$\mathbf{M}_A\ddot{\mathbf{q}} = \mathbf{f}(\mathbf{q}) + \mathbf{f}^{imp} + \mathbf{R}^f \tag{14.14a}$$

$$\mathbf{M}\ddot{\mathbf{d}} = \mathbf{N}^T\mathbf{f}(\mathbf{u}) \tag{14.14b}$$

where $\mathbf{f}^{imp}$ is an impedance force and $\mathbf{R}^f$ is a random force. The impedance force is defined as:

$$\mathbf{f}_i^{imp} = \sum_{j \in neighbors(i)} \int_0^t \Theta_j(t-\tau) \times \left(\mathbf{q}_j(\tau) - \bar{\mathbf{u}}_j(\tau) - \mathbf{R}_j^d(\tau)\right) d\tau \tag{14.15}$$

where $\Theta_j(t-\tau)$ and $\mathbf{R}_j^d(t)$ are a time history kernel and a random displacement term respectively. The purpose of the random force $\mathbf{R}^f$ is to restitute the energy dissipated by the impedance force and thus ensuring energy conservation.

The important point to note in this method is that the impedance force has the role of dissipating the short wavelengths that cannot be represented by the FE mesh. This energy dissipation is based on the generalized Langevin equation (GLE) [73–75]. One limitation is that the time history kernel is usually derived for a given lattice structure which restricts their usage to crystalline materials.

Several other concurrent atomistic-continuum coupled approaches have been developed using the idea of GLE to dissipate short wavelengths that are reflected at the MD-FE interface. However, these approaches differ in the way the time history kernel function $\Theta$ is derived. For instance, Cai et al. [76] computed $\Theta$ from several MD simulations. E and Huang [77, 78] have computed analytically the kernel coefficients by minimizing the reflection coefficients at each wavenumber. Wagner et al. [79] have computed $\Theta$ using the Laplace and the Fourier transforms. Most of these approaches assume the temperature of the coarse scale to be zero to ignore the random force term $\mathbf{R}^f$ and thus are not suitable for thermal transfer applications. A few methods based on the idea of GLE also exists that are suitable for studying problems with non-equilibrium processes. For instance, Karpov et al. [80] have developed a concurrent atomistic continuum model by using analytical expressions for $\Theta$ and including a random force term to allow the passage of thermal energy between the atomistic and continuum regions. Mathew et al. [81] have used a time

dependent friction force and a weighted random force to treat thermal fluxes across the atomistic-continuum interface. The common feature in all these methods is the time history kernel function, which is built using different techniques. Recently, a parametric study focused on the influence of time and spatial kernels on the dynamics of one-dimensional MD systems was conducted [82] and revealed that spatial filters present interesting features, when compared to time filters, which can be exploited as will be demonstrated in a later section.

### *14.3.2 Sliding Friction and Heat Generation*

Sliding friction between rough surfaces generates intense heat fluxes because of the large plastic deformations. This can put to the test any direct multiscale method [83]. For instance, when rough surfaces carved from two cubic-like copper crystals at zero Kelvin with self-affine fractal [84] generated with a Voss [85, 86] algorithm (as presented in Fig. 14.2) are pressed against each other and sled, a temperature rise is to be expected. In order to demonstrate the artificial impact of the Bridging Domain algorithm on sliding contact dynamics, three different models are compared:

- Full MD model (the continuum zone is replaced by atoms and serves as a reference)
- Coupled model (as described in Fig. 14.2)
- Reduced MD model (the continuum zone is eliminated).

To quantify the effect of the coupling with regards to phonon emission, the kinetic energy of the top zone of the deformable body is measured. This zone contains the energy close to the asperities, without any contribution of the overlap region atoms.

These measures are presented in Fig. 14.3. The coupled approach always leads to a minimal residual kinetic energy, while the reduced case stores a lot more vibrational energy in the contacting zone. It is noteworthy that the coupling scheme fails in recovering the full MD behavior: the kinetic energy profile remains almost flat and at a low value.

Interestingly, most work in the literature has sought to prevent wave reflections without necessarily considering that the damping of the problematic (high frequency) waves could impact the uncoupled zones. Indeed, the Bridging Domain method, when handling properly the undesired high frequency waves incoming from the molecular domain, is damping a part of the kinetic energy in an ad hoc way [70, 87]. Here, with an initial state of zero Kelvin, and with asperities of various sizes and shapes, colliding and scratching at contact points, thermal vibrations are being generated at an important rate. The resulting heat increase is an integral part of the contact problem and for some problems should not be damped entirely by the coupling zone. Thus, the sliding friction problem calls for a thermo-mechanical multiscale model with the potential to address heat fluxes.

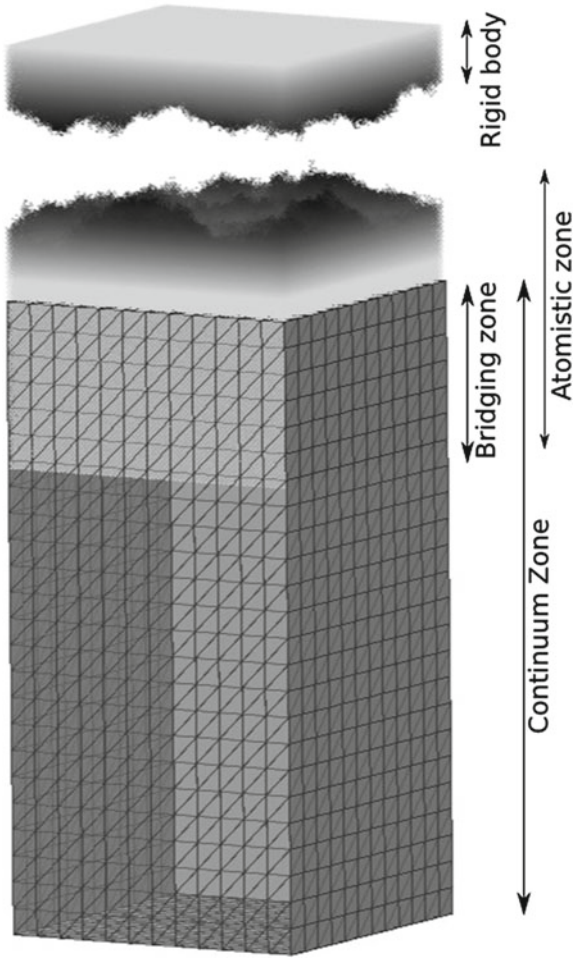


**Fig. 14.2** 3D View of the mesh and atomic zone coupled together

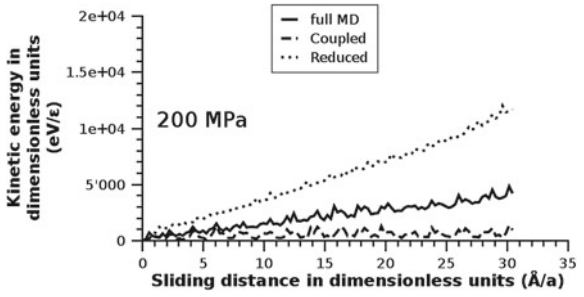


**Fig. 14.3** Residual kinetic energy in the zone near contacting asperities (thickness 24 a, a = 3.615Å is the lattice constant) for the full MD (*solid line*), coupled (*dashed line*) and reduced cases (*dotted line*)

## 14.4 Finite Temperature Coupling

This section begins with the description of a novel multiscale model coupling MD and FE. A scale transfer operator using a spatial filter is described. Then the coupling formulation, which uses GLE to damp selective frequency modes in the coupling region, is presented. Later on, the thermal coupling formulation to treat thermal fluxes across the MD-FE interface is introduced.

In order to illustrate the geometry of the coupling zone needed for this strategy, a schematic is presented in Fig. 14.4. $\Omega^A$ and $\Omega^C$ are used to refer to the pure atomistic and the pure continuum regions, while $\Omega^{C(A)}$ and $\Omega^{A(C)}$ represent the coupling and boundary regions respectively [49, 88].

While the dynamics of an atom in region $\Omega^A$ follow the classical Newtonian equation, the mechanical and thermal fields within the continuum model are represented with two different partial differential equations: the evolution of the displacement field is described using the equations of motion combined with a linear elastic law, while Fourier's thermal conductivity equations are called upon to represent the temperature field. It should be noted that the heat propagation within the system is assumed to be only due to conduction without taking into account convection and radiation. The dynamics inside the coupling $\Omega^{A(C)}$ and the boundary $\Omega^{C(A)}$ regions, where both atoms and finite elements coexist, need three components such as a *scale transfer operator*, a *selective thermostat* and a *heat balance equation*, which are presented in the following sections.

### *14.4.1 Scale Transfer Operator*

In the boundary region $\Omega^{A(C)}$, the atomic displacements and velocities are simply computed from the interpolated FE fields, whereas the coupling is more complex when information has to pass from the fine to the coarse scale. For this operation, a scale transfer operator is used to define the transmission of information, such as

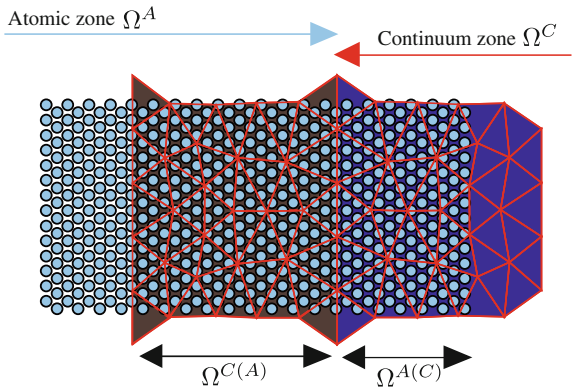


**Fig. 14.4** Illustration of the MD-FE multiscale domain

displacement and velocity, from one length scale to another without corrupting the system dynamics in either of the scales.

For example, Fackeldey et al. [89, 90] have developed an atomistic-continuum coupled approach using a weighted least square projection as a scale transfer operator to decompose the atomic displacements into low and high frequency components. They provided numerical examples demonstrating the seamless transmission of displacements from MD to FE at zero Kelvin. However, it can be shown that the least square projection has poor filtering properties [91].

In order to improve this scale transfer operator, a least-square projection can be combined [91] with a spatial filter to define an improved scale transfer operator. The continuum displacement $U_J$ of any node $J$ in the coupling region $\Omega^{C(A)}$ is then formally obtained with:

$$U_J = \sum_I A^{-1}_{I,J} \sum_{i \in \Omega^{C(A)}} \hat{u}_i \, N_I(X_i) \tag{14.16}$$

$$\text{with } A_{I,J} = \sum_{i \in \Omega^{C(A)}} N_I(X_i) N_J(X_i)$$

where $A_{I,J}$ is the least square projection matrix [40], $N_I$ is the shape function described by a linear polynomial for node I and $\hat{u}_i$ is the spatially filtered displacement of any atom $i$ inside the $\Omega^{C(A)}$ region defined by:

$$\hat{u}_i = \sum_{j \in neighbors(i)} \gamma(|X_i - X_j|) u_j \tag{14.17}$$

where $\gamma$ is a spatial filter (memory kernel) function, which can be chosen so that the *finite elements* receive only waves for which they have enough degrees of freedom to represent. The continuum velocity field is defined in a similar manner. The scale transfer operator hence defined allows to transmit precisely the band of frequencies that the mesh can handle with its coarser representation. The waves not mechanically transmitted have to be transformed into thermal energy which would allow the coupling of heat fluxes. This is the role of the selective thermostat presented below.

### *14.4.2 Selective Thermostat*

The presented method stands on the generalized Langevin equation (GLE) [73–75]. The dynamics of atoms inside the coupling region is described using the GLE which incorporates spatial filters as expressed by the following equations:

$$m\dot{v} = -\nabla\Phi - \frac{m(v - \hat{v})}{\alpha} + R \tag{14.18}$$

where $m$ is the mass, $v$ is the velocity, $\dot{v}$ is the acceleration, $\hat{v}$ is the spatially filtered velocity and $\Phi$ is the potential function. The second term on the right side of equation (14.18) is the frictional force, $\alpha$ is a damping parameter to decide the strength of the frictional force, and $R$ is a random or fluctuating force which is correlated in both space and time. The purpose of the random force is to balance both the energy dissipation of the friction force and the heat exchange with the continuum model. For instance the random force $R(x,t)$ can be derived analytically for a one-dimensional mono-atomic lattice:

$$R(x,t) = \frac{1}{\alpha}\sqrt{\frac{2mk_BT}{N}}\sum_k cos(\omega(k)t + k\,x + \phi(k)) \tag{14.19}$$

where $k_B$ is the Boltzmann constant, $T$ is the desired temperature, $N$ is the number of restitution modes, $\phi(k)$ is a random phase sampled in the interval $[0, 2\pi]$ and $\omega(k)$ is the angular frequency associated with the wave vector $k$, taken from the dispersion relation. In the restitution, a temperature $T$ has to be defined.

In the case of thermal equilibrium, the temperature $T$ can be taken as a constant. However, in the non-equilibrium case, this temperature is given by the continuum model and ensures that the continuum can exchange heat with the atomic region. As an additional component, the energy balance presented in next section allows heat fluxes to be introduced in the continuum.

### *14.4.3 Heat Balance Equation*

The governing equation used to describe the thermal transfer assuming Fourier's law ($\mathbf{q} = -\kappa\,\nabla T$) within the finite-element model is given by:

$$\rho\,C_v\,\dot{T} = \nabla\cdot(\kappa\,\nabla T) + Q \tag{14.20}$$

where $\rho$ is the mass density, $C_v$ is the specific heat capacity, $\dot{T}$ is the temperature rate, $\kappa$ is the thermal conductivity, $T$ is the temperature and $Q$ is the volumetric heat source per unit time. Classically [17, 18], the finite element resolution of (14.20) leads to:

$$\mathbf{C}_{IJ}\dot{T}_J + \mathbf{K}_{IJ}T_J = Q_I \tag{14.21}$$

with $\mathbf{C}$ the capacity matrix, $\mathbf{K}$ the conductivity matrix and $Q_I$ the heat rate associated with node $I$ which is described as:

$$Q_I = \int_{\Omega^{C(A)}} N_I\,Q\,d\Omega^C \tag{14.22}$$

where $N_I$ is the shape function associated with node $I$. The balance of the thermal energy inside the $\Omega^{C(A)}$ region is achieved from the difference between the heat rate of the atomistic and the continuum models as described by:

$$Q(x) = \sum_{i \in \Omega^{C(A)}} (q_i^F - q_i^R)\, \delta(x - x_i) \tag{14.23}$$

where $\delta(x - x_i)$ is the Dirac delta function equal to infinity at the position $x_i$ of an atom $i$ and zero elsewhere, $q_i^F$ and $q_i^R$ are the per atom heat rate due to the friction and random forces respectively, which are expressed as:

$$q_i^F = \frac{1}{\alpha}\, m\, (v - \hat{v})\, v_i \qquad q_i^R = R_i\, v_i \tag{14.24}$$

Thus, the heat rate $Q_I$ associated with node $I$ is expressed as:

$$Q_I = \int_{\Omega^{C(A)}} N_I\, Q d\Omega^C = \sum_{i \in C(A)} N_I(x_i)\, (q_i^F - q_i^R) \tag{14.25}$$

Because of the shape functions scope, only interface nodes will receive a flux coming from the MD model, which turns out to be a boundary condition for the FE region.

## 14.5 Validation and Application

In this section, three different numerical examples illustrate the method. In the first example, the method is validated by passing a mechanical wave pulse while maintaining the system at a constant finite temperature. The second example includes a mechanical wave propagation from the FE region into the MD region in addition to transient heat propagation. Finally, the case of a dynamic contact is shown.

In what follows, the material is a FCC aluminum crystal thin sheet which has a hexagonal lattice corresponding to the (111) plane of bulk aluminum. We resort to a simple harmonic potential with first neighbor interactions to prevent any plastic deformation. For the continuum model, the equations of motion described by an elastic orthotropic material law and the Fourier's heat conduction law are used to describe mechanical and thermal fields respectively. The parameters for both MD and FE models are found in Tables 14.1 and 14.2.

As previously stated, the dispersion relation between the angular frequency $\omega(k_x, k_y, b)$ and the wave vector $\mathbf{k}$ is called upon to construct the random force $R(\mathbf{x}, t)$. In the case of the considered two-dimensional hexagonal lattice it follows:

**Table 14.1** Parameters of the MD model

| Parameters | Value |
|---|---|
| $m$ | 26.98 g.mol$^{-1}$ |
| $\varepsilon$ | 1.36 Kcal.mol$^{-1}$ |
| $\sigma$ | 2.54 Å |
| $r_0$ | $2.016\sqrt{2}$ Å |
| $r_1$ | $\sqrt{3}r_0$ Å |
| $r_{cut}$ | 3.89 Å |

**Table 14.2** Parameters of the FE model

| Parameters | Value |
|---|---|
| $\rho$ | 3.83 g.mol$^{-1}$.Å$^{-2}$ |
| $E1$ | 9.78 Kcal.mol$^{-1}$.Å$^{-3}$ |
| $E2$ | 9.78 Kcal.mol$^{-1}$.Å$^{-3}$ |
| $\nu 12$ | 0.33 |
| $G12$ | 3.67 Kcal.mol$^{-1}$.Å$^{-3}$ |
| $C_v$ | 1.47e$^{-4}$ Kcal.g$^{-1}$.$K^{-1}$ |
| $\kappa$ | 1.23e$^{-3}$ Kcal.mol$^{-1}$.Å$^{-1}$.$fs^{-1}$.$K^{-1}$ |

$$\omega^2(k_x, k_y, b) = \frac{C}{m}\Bigg[3 - \cos(k_x) - 2\zeta + (-1)^b \sqrt{(\cos(k_x) - \zeta)^2 + 3\sin^2\left(\frac{k_x}{2}\right)\sin^2\left(\frac{\sqrt{3}k_y}{2}\right)}\Bigg] \tag{14.26}$$

where $\zeta = \cos\left(\frac{k_x}{2}\right)\cos\left(\frac{\sqrt{3}k_y}{2}\right)$, $b$ is the acoustic branch number, $\mathbf{k} = (k_x, k_y)$ is the wave vector and $m$ is the mass of each atom.

### *14.5.1 Mechanical Wave Propagation at Finite Temperature*

The coupled model is shown in Figure 14.5. The dimensions of the MD region ($\Omega^A$) is $400r_0 \times 40r_1$, where $r_0$ is the inter-atomic spacing and $r_1 = \frac{\sqrt{3}}{2}r_0$. Two FE meshes each with 3520 linear triangular elements with a characteristic size $h = 5.0r_0$, as shown in Fig. 14.5, are used on either side of the MD region. Periodic boundary conditions are imposed along the y-direction for both models. Along the x-direction the size of the coupling region $\Omega^{C(A)}$ is $20r_0$. Each coupling region contains 4 and 16 finite elements along x and y directions respectively. A boundary region with 8 finite elements along x direction on both ends of $\Omega^A$ is used. For the initial condition, a

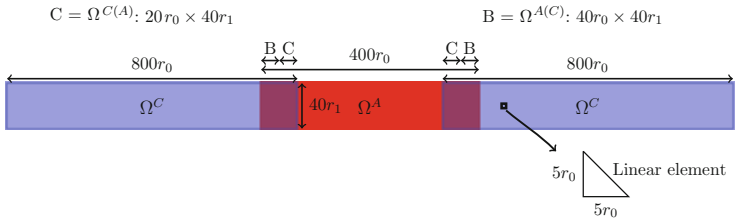


**Fig. 14.5** Illustration of the coupled model. A uniform FE mesh with linear triangle elements is used on either side of the MD region

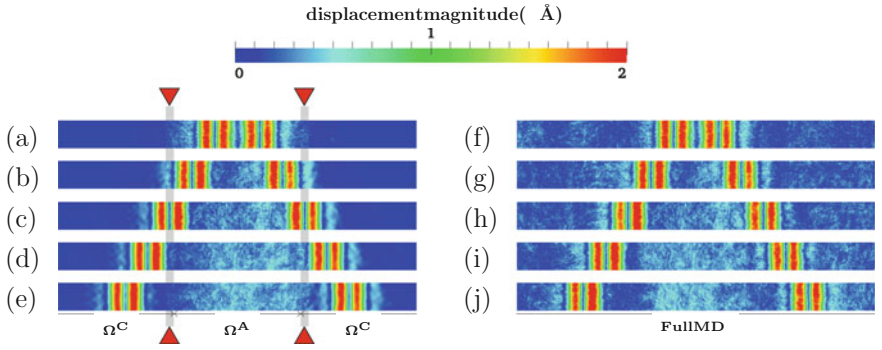


**Fig. 14.6** Comparison of the displacement field in the coupled model (*Left*) with the full MD simulation (*Right*) at time $t = 4$, 8, 12, 16 and 20 ps. The temperature of the system is maintained at 50 K. The overlap region in the coupled model is indicated using the *triangle marks* in *red color*. For the sake of visualization, only 50 % of the complete mesh on either side of the MD region is shown

low frequency wave packet is introduced in the region $\Omega^A$, while the high frequency modes in the MD region are only due to the injected temperature which is set to 50 K. The energy dissipated in the coupling region due to the damping is balanced by the random force.

The displacement profiles extracted from the coupled simulation with those obtained from the full MD results are compared in Fig. 14.6 and show a good agreement.

As expected the small wavelengths are damped and restituted in the coupling region with the help of a spatial filter. This ensures that the energy of the entire model, i.e. the sum of kinetic, potential and thermal energies, remains constant during the entire simulation [91].

### *14.5.2 Thermo-Mechanical Wave Propagation*

In this example, a transient heat problem superposed with an impulse wave is considered to validate the coupling approach in the case of non-equilibrium processes. Figure 14.7, shows the MD-FE coupled model used in this example.

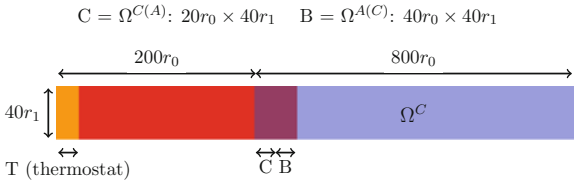


**Fig. 14.7** Setup of the coupled model with a thermostat at 200 K imposed on a group of atoms on the left side of the MD region

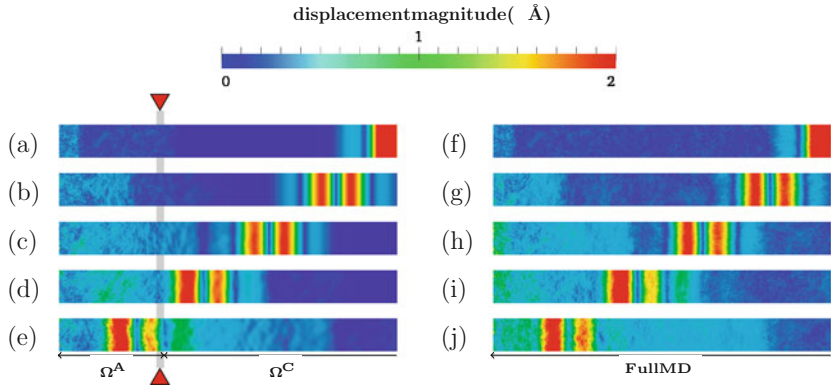


**Fig. 14.8** Comparison of the displacement field in the coupled model (*Left*) with the full MD simulation (*Right*) at time $t = 0$, 10, 20, 30 and 40 ps. The overlap region in the coupled model is indicated using the *triangle marks* in *red* color

The size of the MD region $\Omega^A$ is $200r_0 \times 40r_1$, composed of 16,000 atoms. Similarly to the previous example, triangular finite elements ($h = 5r_0$) are used to represent the coarse scale model. Furthermore, the coupling and boundary regions share similar sizes with the previous example.

An initial temperature of 10 K is imposed everywhere in the model. Then, a Langevin thermostat of temperature 200 K is applied on a group of 3200 atoms on the left side of the MD region. The thermostat creates a thermal flux within the entire system which initiates transient heat propagation from the MD to FE region. At the same time, an impulse wave is imposed on the right side of the FE region. The dynamics of the entire system is allowed to evolve for a total time of 50 ps.

The snapshots of the displacement profile of the coupled MD–FE model and of the full MD simulations are shown in Fig. 14.8. A smooth transition of the large wavelength from the FE to the MD region can be observed. In addition to the displacements, the time averaged temperature profiles for both the coupled and the full MD models at time $t = 50$ ps are shown in Fig. 14.9a. Also, the total energy of the coupled model is compared with the full MD simulation and found to be in good agreement (see Fig. 14.9b).

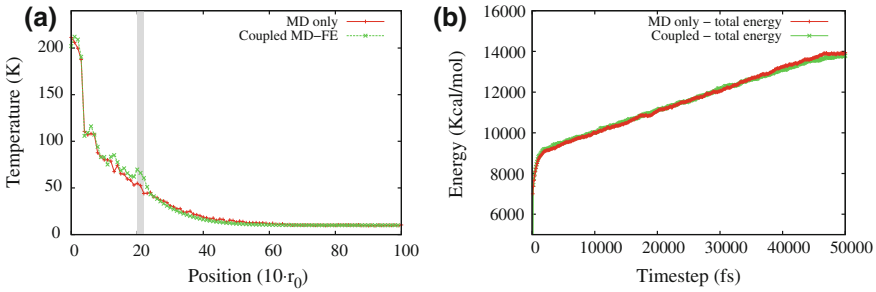


**Fig. 14.9** **a** Comparison of the temperature profile of the coupled model with the full MD simulation at time $t = 50$ ps. The overlap region is indicated with a *light gray* background. **b** Comparison of the total energy of the coupled model with the full MD simulation. The total energy increases with time as it is a non-equilibrium process

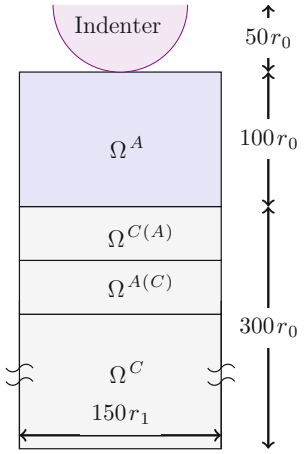


**Fig. 14.10** Illustration of the multiscale model used for dynamic contact

### *14.5.3 Application to Dynamic Contact*

Once again, the aluminum material from the previous two examples is considered to model the deformable substrate, which is subjected to an impact by a rigid circular indenter of radius $50r_0$. The schematic of the coupled MD–FE model is shown in Fig. 14.10. An initial temperature of $T = 20$ K is set within the MD–FE model. After reaching thermal equilibrium, the indenter impacts the substrate at a velocity of 5 Å.ps$^{-1}$.

The displacement profile of the MD–FE model is extracted at various timesteps and compared with the displacement profile of a full MD model as shown in Fig. 14.11. Again, a good agreement with the reference full MD is achieved. During the impact, the indenter tip creates waves propagating into the substrate. Waves with large wavelengths propagate through the FE mesh, while high frequency waves that cannot be represented by the FE mesh are transmitted as a thermal flux. Thus, the

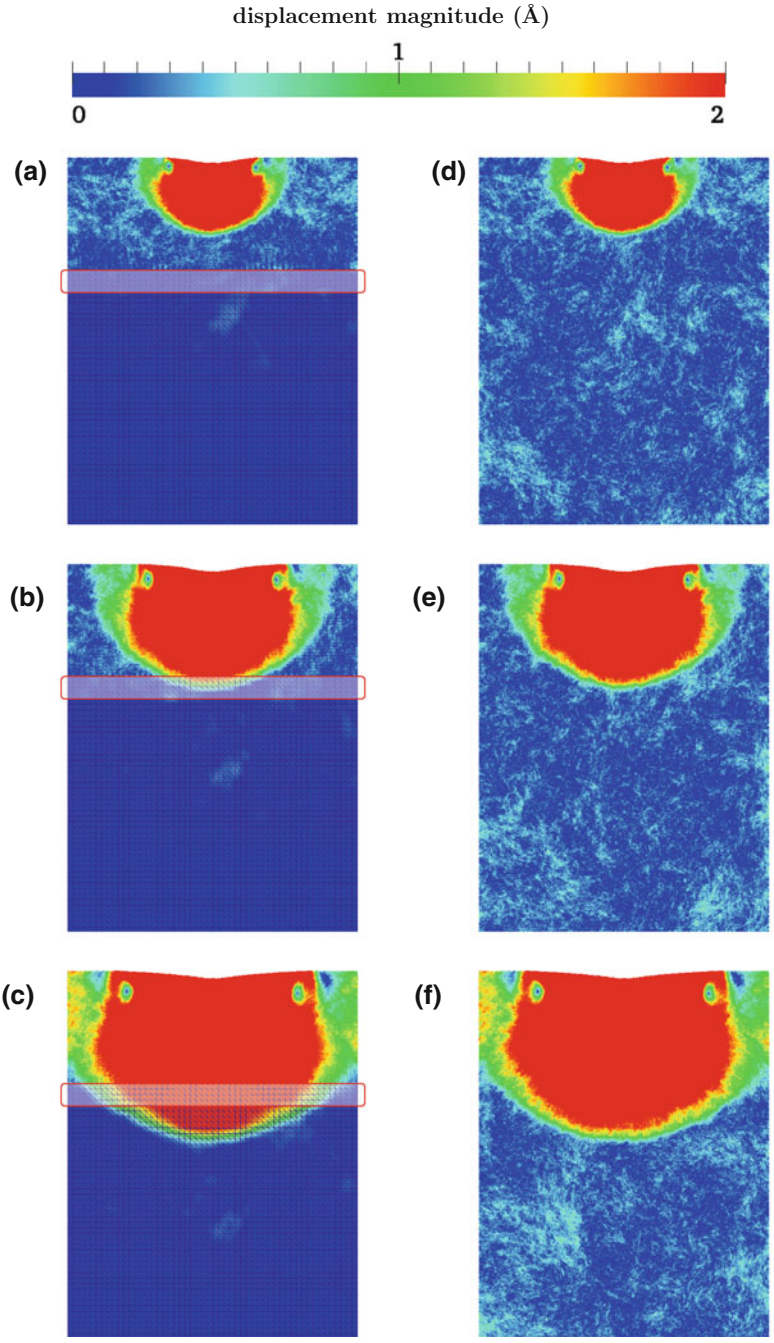


**Fig. 14.11** Snapshots of the displacement field in the coupled model (*Left*) and the full MD model (*Right*) at time $t = 6$, 9 and 12 ps. The overlap region in the coupled model is shown using a transparent rectangle

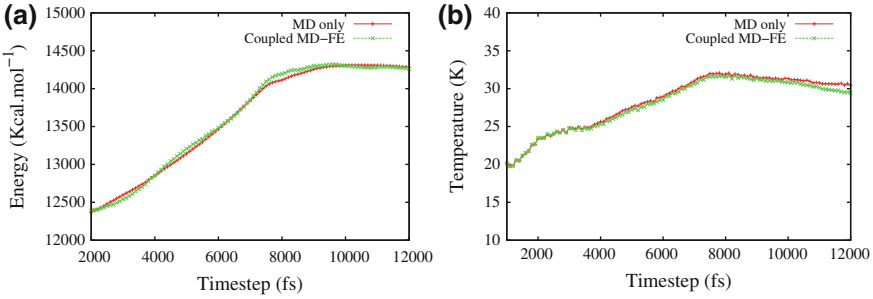


**Fig. 14.12** **a** Total energy comparison between the coupled model and the full MD simulation and **b** Temperature in the MD region ($\Omega^A$) in the coupled and the full MD models

total energy of the coupled model is found to be in good match with the full atomistic solution as shown in Fig. 14.12a. The atomistic temperature in region ($\Omega^A$) is also measured for the coupled and the full MD models, which is found to have a reasonable agreement as shown in Fig. 14.12b. Thus, the proposed coupling approach can be applied to a dynamic contact problem and produce satisfactory results.

## 14.6 Conclusion

This chapter discussed modeling techniques of contact at the nanoscale with a special emphasis on molecular dynamics. The limitations of single scale approaches motivated the development of multiscale methods. A review on the state-of-the-art multiscale methods was presented, which was followed by a discussion brought by a rough-on-rough sliding problem simulated using a now classical coupling method (Bridging Domain method). The influence of the coupling scheme was quantified by measuring the kinetic energy of atoms close to the asperities and was compared with a full MD and a reduced MD models. The results show clearly that an ad-hoc damping of high frequency waves changes the dynamics of sliding friction. This is an important limitation of most current multiscale approaches, and prevents their wide usage in sliding contact simulations, in which one expects large thermal fluxes to be generated.

Consequently, an alternative multiscale approach was proposed to concurrently couple molecular dynamics and a finite element model at finite temperatures. The proposed approach is based on the generalized Langevin equation and resorts to spatial filters. The thermal coupling that handles the heat flux between the atomistic and continuum models was presented. The fundamental idea is that the high frequency waves that are not represented by the finite elements are damped by the friction force through spatial filtering. The balance with the damped energy is performed through the random force. Finally, we presented two-dimensional numerical examples: i) wave propagation at constant finite temperature, ii) thermo-mechanical wave

propagation, and iii) a dynamic contact problem. In all cases the coupled simulations were compared with full MD simulations and found to be in good agreement. While finite-temperature multiscale approaches show great prospect for friction simulations, it is important to emphasize that more research is needed to improve the computing performance (especially in three dimensions), and to explore the thermomechanical mechanisms contributing to friction within this new framework.

**Acknowledgments** This material is based on the work supported by the Swiss National Foundation under Grant no 200021_122046/1 and the European Research Council Starting Grant no 240332.

## References

1. H. Czichos, *Tribology* (Elsevier, Amsterdam 1978)
2. A. Majumdar, B. Bhushan, Role of fractal geometry in roughness characterization and contact mechanics of surfaces. J. Tribol. **112**(2), 205–216 (1990)
3. B.N.J. Persson, Contact mechanics for randomly rough surfaces. Surf. Sci. Rep. **61**(4), 201–227 (2006)
4. S.B. Ramisetti, C. Campa, Anciaux, J.F. Molinari, M.H. Mser, M.O. Robbins, The autocorrelation function for island areas on self-affine surfaces. J. Phys. Condens. Matter **23**(21), 215004 (2011)
5. B. Luan, M.O. Robbins, The breakdown of continuum models for mechanical contacts. Nature **435**(7044), 929–932 (2005)
6. G.V. Dedkov, Experimental and theoretical aspects of the modern nanotribology. Phys. Status Solidi A **179**(1), 375 (2000)
7. J. Gao, W.D. Luedtke, D. Gourdon, M. Ruths, J.N. Israelachvili, U. Landman, Frictional forces and Amontons' law: From the molecular to the macroscopic scale. J. Phys. Chem. B **108**(11), 3410–3425 (2004)
8. J.O. Koskilinna, M. Linnolahti, T.A. Pakkanen, Friction coefficient for hexagonal boron nitride surfaces from ab initio calculations. Tribol. Lett. **24**(1), 37–41 (2006)
9. M. Renouf, F. Massi, N. Fillot, A. Saulot, Numerical tribology of a dry contact. Tribol. Int. **44**(78), 834–844 (2011)
10. J.F. Jerier, J.F. Molinari, Normal contact between rough surfaces by the discrete element method. Tribol. Int. **47**, 1–8 (2012)
11. V.S. Deshpande, A. Needleman, E. Van der Giessen, Discrete dislocation plasticity analysis of static friction. Acta Mater. **52**(10), 3135–3149 (2004)
12. S. Hyun, L. Pei, J.F. Molinari, M.O. Robbins, Finite-element analysis of contact between elastic self-affine surfaces. Phys. Rev. E **70**(2), 026117 (2004)
13. P. Wriggers, T.A. Laursen, *Computational Contact Mechanics* (Springer, Dordrecht, 2008)
14. B. Luan, M.O. Robbins, Contact of single asperities with varying adhesion: Comparing continuum mechanics to atomistic simulations. Phys. Rev. E **74**(2), 026111 (2006)
15. Y. Mo, I. Szlufarska, Roughness picture of friction in dry nanoscale contacts. Phys. Rev. B **81**(3), 035405 (2010)
16. P. Spijker, G. Anciaux, J.F. Molinari, The effect of loading on surface roughness at the atomistic level. Comput. Mech. **50**(3), 273–283 (2011)
17. T.J.R. Hughes, *The Finite Element Method: Linear Static and Dynamic Finite Element Analysis* (Dover Publications, New York, 2000)
18. O.C. Zienkiewicz, R.L. Taylor, J.Z. Zhu, *The Finite Element Method: Its Basis & Fundamentals* (Elsevier Butterworth-Heinemann, Amsterdam, 2005)
19. D.C. Rapaport, *The Art of Molecular Dynamics Simulation* (Cambridge University Press, 2004)

20. K. Komvopoulos, J. Yang, Dynamic analysis of single and cyclic indentation of an elasticplastic multi-layered medium by a rigid fractal surface. J. Mech. Phys. Solids **54**(5), 927–950 (2006)
21. K. Komvopoulos, Z.Q. Gong, Stress analysis of a layered elastic solid in contact with a rough surface exhibiting fractal behavior. Int. J. Solids Struct. **44**(78), 2109–2129 (2007)
22. K. Komvopoulos, Effects of multi-scale roughness and frictional heating on solid body contact deformation. C. R. Mnique **336**(12), 149–162 (2008)
23. S. Hyun, M.O. Robbins, Elastic contact between rough surfaces: Effect of roughness at large and small wavelengths. Tribol. Int. **40**(10–12), 1413–1422 (2007)
24. H.J.C. Berendsen, *Simulating the Physical World: Hierarchical Modeling from Quantum Mechanics to Fluid Dynamics* (Cambridge University Press, 2007)
25. M. Griebel, S. Knapek, G. Zumbusch, *Numerical Simulation in Molecular Dynamics: Numerics, Algorithms, Parallelization, Applications* (Springer, November 2010)
26. J. Rottler, M.O. Robbins, Macroscopic friction laws and shear yielding of glassy solids. Comput. Phys. Commun. **169**(13), 177–182 (2005)
27. O.M. Braun, A.G. Naumovets, Nanotribology: Microscopic mechanisms of friction. Surf. Sci. Rep. **60**(67), 79–158 (2006)
28. H.H. Yu, P. Shrotriya, Y.F. Gao, K.S. Kim, Micro-plasticity of surface steps under adhesive contact: Part I surface yielding controlled by single-dislocation nucleation. J. Mech. Phys. Solids **55**(3), 489–516 (2007)
29. C. Campañá, M.H. Müser, Contact mechanics of real vs. randomly rough surfaces: a Green's function molecular dynamics study. EPL (Europhysics Letters) **77**(3), 38005 (2007)
30. H.J. Kim, W.K. Kim, M.L. Falk, D.A. Rigney, MD simulations of microstructure evolution during high-velocity sliding between crystalline materials. Tribol. Lett. **31**(1), 67–67 (2008)
31. C. Yang, B.N.J. Persson, Contact mechanics: contact area and interfacial separation from small contact to full contact. J. Phys.: Condens. Matter **20**(21), 215214 (2008)
32. T. Liu, G. Liu, P. Wriggers, S. Zhu, Study on contact characteristic of nanoscale asperities by using molecular dynamics simulations. J. Tribol. **131**(2), 022001–022001 (2009)
33. P. Spijker, G. Anciaux, J.F. Molinari, Dry sliding contact between rough surfaces at the atomistic scale. Tribol. Lett. **44**(2), 279–285 (2011)
34. P. Spijker, G. Anciaux, J.F. Molinari, Relations between roughness, temperature and dry sliding friction at the atomic scale. Tribol. Int. **59**, 222–229 (2013)
35. F.F. Abraham, R. Walkup, H. Gao, M. Duchaineau, T.D.D.L. Rubia, M. Seager, Simulating materials failure by using up to one billion atoms and the world's fastest computer: workhardening. Proc. Nat. Acad. Sci. **99**(9), 5783–5787 (2002)
36. J. Broughton, F. Abraham, N. Bernstein, E. Kaxiras, Concurrent coupling of length scales: Methodology and application. Phys. Rev. B **60**(4), 2391–2403 (1999)
37. R. Miller, E.B. Tadmor, R. Phillips, M. Ortiz, Quasicontinuum simulation of fracture at the atomic scale. Modell. Simul. Mater. Sci. Eng. **6**(5), 607–638 (1998)
38. V.B. Shenoy, R. Miller, E.B. Tadmor, R. Phillips, M. Ortiz, Quasicontinuum models of interfacial structure and deformation. Phys. Rev. Lett. **80**(4), 742–745 (1998)
39. W.A. Curtin, R.E. Miller, Atomistic/continuum coupling in computational materials science. Modell. Simul. Mater. Sci. Eng. **11**(3), R33–R68 (2003)
40. W.K. Liu, E.G. Karpov, S. Zhang, H.S. Park, An introduction to computational nanomechanics and materials. Comput. Methods Appl. Mech. Eng. **193**(17–20), 1529–1578 (2004)
41. H.S. Park, W.K. Liu, An introduction and tutorial on multiple-scale analysis in solids. Comput. Methods Appl. Mech. Eng. **193**(17–20), 1733–1772 (2004)
42. G. Lu, E. Kaxiras, *An overview of multiscale simulations of materials. Handbook of Theoretical and Computational Nanotechnology* (American Scientific Publishers, Stevenson Ranch, 2005), p. 10
43. R.E. Miller, E.B. Tadmor, A unified framework and performance benchmark of fourteen multiscale atomistic/continuum coupling methods. Modell. Simul. Mater. Sci. Eng. **17**(5), 053001 (2009)
44. J.M. Wernik, S.A. Meguid, Coupling atomistics and continuum in solids: status, prospects, and challenges. Int. J. Mech. Mater. Des. **5**(1), 79–110 (2009)

45. E. Weinan, B. Engquist, X. Li, W. Ren, E. Vanden-Eijnden, Heterogeneous multiscale methods: a review. Commun. Comput. Phys. **2**(3), 367–450 (2007)
46. E.B. Tadmor, M. Ortiz, R. Phillips, Quasicontinuum analysis of defects in solids. Philos. Mag. A **73**(6), 1529–1563 (1996)
47. R. Miller, E.B. Tadmor, The quasicontinuum method: overview, applications and current directions. J. Comput. Aided Mater. Des. **9**(3), 203–239 (2002)
48. L.E. Shilkrot, R.E. Miller, W.A. Curtin, Coupled atomistic and discrete dislocation plasticity. Phys. Rev. Lett. **89**(2), 025501 (2002)
49. S.P. Xiao, T. Belytschko, A bridging domain method for coupling continua with molecular dynamics. Comput. Methods Appl. Mech. Eng. **193**(17–20), 1645–1669 (2004)
50. S. Kohlhoff, P. Gumbsch, H.F. Fischmeister, Crack propagation in b.c.c. crystals studied with a combined finite-element and atomistic model. Philos. Mag. A **64**(4), 851–878 (1991)
51. G.J. Wagner, W.K. Liu, Coupling of atomistic and continuum simulations using a bridging scale decomposition. J. Comput. Phys. **190**(1), 249–274 (2003)
52. R. Miller, M. Ortiz, R. Phillips, V. Shenoy, E.B. Tadmor, Quasicontinuum models of fracture and plasticity. Eng. Fract. Mech. **61**(3–4), 427–444 (1998)
53. V.B. Shenoy, R. Miller, E.B. Tadmor, D. Rodney, R. Phillips, M. Ortiz, An adaptive finite element approach to atomic-scale mechanicsthe quasicontinuum method. J. Mech. Phys. Solids **47**(3), 611–642 (1999)
54. J. Knap, M. Ortiz, An analysis of the quasicontinuum method. J. Mech. Phys. Solids **49**(9), 1899–1923 (2001)
55. V. Shenoy, V. Shenoy, R. Phillips, Finite temperature quasicontinuum methods. MRS Online Proc. Libr. **538** (1998)
56. L.M. Dupuy, E.B. Tadmor, R.E. Miller, R. Phillips, Finite-temperature quasicontinuum: molecular dynamics without all the atoms. Phys. Rev. Lett. **95**(6), 060202 (2005)
57. Z. Tang, H. Zhao, G. Li, N.R. Aluru, Finite-temperature quasicontinuum method for multiscale analysis of silicon nanostructures. Phys. Rev. B **74**(6), 064110 (2006)
58. Y. Kulkarni, J. Knap, M. Ortiz, A variational approach to coarse graining of equilibrium and non-equilibrium atomistic description at finite temperature. J. Mech. Phys. Solids **56**(4), 1417–1449 (2008)
59. J. Marian, G. Venturini, B.L. Hansen, J. Knap, M. Ortiz, G.H. Campbell, Finite-temperature extension of the quasicontinuum method using langevin dynamics: entropy losses and analysis of errors. Modell. Simul. Mater. Sci. Eng. **18**(1), 015003 (2010)
60. E.B. Tadmor, F. Legoll, W.K. Kim, L.M. Dupuy, R.E. Miller, Finite-temperature quasicontinuum. Appl. Mech. Rev. **65**(1), 010803–010803 (2013)
61. L.E. Shilkrot, W.A. Curtin, R.E. Miller, A coupled atomistic/continuum model of defects in solids. J. Mech. Phys. Solids **50**(10), 2085–2106 (2002)
62. E. Van der Giessen, A. Needleman, Discrete dislocation plasticity: a simple planar model. Modell. Simul. Mater. Sci. Eng. **3**(5), 689 (1995)
63. B. Shiari, R.E. Miller, W.A. Curtin, Coupled atomistic/discrete dislocation simulations of nanoindentation at finite temperature. J. Eng. Mater. Technol. **127**(4), 358–368 (2005)
64. S. Qu, V. Shastry, W.A. Curtin, R.E. Miller, A finite-temperature dynamic coupled atomistic/discrete dislocation method. Modell. Simul. Mater. Sci. Eng. **13**(7), 1101 (2005)
65. H.B. Dhia, Problémes mécaniques multi-échelles: la méthode arlequin. Comptes Rendus de l'Académie des Sciences - Series IIB - Mechanics-Physics-Astronomy, 326(12):899–904 (1998)
66. H.B. Dhia, G. Rateau, The arlequin method as a flexible engineering design tool. Int. J. Numer. Meth. Eng. **62**(11), 14421462 (2005)
67. P.T. Bauman, H.B. Dhia, N. Elkhodja, J.T. Oden, S. Prudhomme, On the application of the arlequin method to the coupling of particle and continuum models. Comput. Mech. **42**(4), 511–530 (2008)
68. S. Prudhomme, H.B. Dhia, P.T. Bauman, N. Elkhodja, J.T. Oden, Computational analysis of modeling error for the coupling of particle and continuum models by the arlequin method. Comput. Methods Appl. Mech. Eng. **197**(4142), 3399–3409 (2008)

69. T. Belytschko, S.P. Xiao, Coupling methods for continuum model with molecular model. Int. J. Multiscale Comput. Eng. **1**(1), 115–126 (2003)
70. G. Anciaux, O. Coulaud, J. Roman, G. Zerah, *Ghost force reduction and spectral analysis of the 1D bridging method*, Technical report (INRIA, HAL, 2008)
71. G. Anciaux, S.B. Ramisetti, J.F. Molinari, A finite temperature bridging domain method for MD-FE coupling and application to a contact problem. Comput. Methods Appl. Mech. Eng. **205208**, 204212 (2011)
72. H.S. Park, E.G. Karpov, P.A. Klein, W.K. Liu, Three-dimensional bridging scale analysis of dynamic fracture. J. Comput. Phys. **207**(2), 588–609 (2005)
73. S.A. Adelman, Generalized langevin equation approach for atom/solid-surface scattering: collinear atom/harmonic chain model. J. Chem. Phys. **61**(10), 4242–4246 (1974)
74. S.A. Adelman, Generalized langevin theory for gas/solid processes: dynamical solid models. J. Chem. Phys. **65**(9), 3751–3762 (1976)
75. S.A. Adelman, Generalized langevin equation approach for atom/solid-surface scattering: general formulation for classical scattering off harmonic solids. J. Chem. Phys. **64**(6), 2375–2389 (1976)
76. W. Cai, M. de Koning, V.V. Bulatov, S. Yip, Minimizing boundary reflections in coupled-domain simulations. Phys. Rev. Lett. **85**(15), 3213–3216 (2000)
77. E. Weinan, Z. Huang, Matching conditions in atomistic-continuum modeling of materials. Phys. Rev. Lett. **87**(13), 135501 (2001)
78. E. Weinan, Z. Huang, A dynamic atomisticcontinuum method for the simulation of crystalline materials. J. Comput. Phys. **182**(1), 234–261 (2002)
79. G.J. Wagner, E.G. Karpov, W.K. Liu, Molecular dynamics boundary conditions for regular crystal lattices. Comput. Methods Appl. Mech. Eng. **193**(1720), 1579–1601 (2004)
80. E.G. Karpov, H.S. Park, W.K. Liu, A phonon heat bath approach for the atomistic and multiscale simulation of solids. Int. J. Numer. Meth. Eng. **70**(3), 351–378 (2007)
81. N. Mathew, R.C. Picu, M. Bloomfield, Concurrent coupling of atomistic and continuum models at finite temperature. Comput. Methods Appl. Mech. Eng. **200**(5–8), 765–773 (2011)
82. S.B. Ramisetti, G. Anciaux, J.F. Molinari, Spatial filters for bridging molecular dynamics with finite elements at finite temperatures. Comput. Methods Appl. Mech. Eng. **253**, 28–38 (2013)
83. G. Anciaux, J.F. Molinari, Sliding of rough surfaces and energy dissipation with a 3D multiscale approach. Int. J. Numer. Meth. Eng. **83**(8–9), 1255–1271 (2010)
84. B.N.J. Persson, O. Albohr, U. Tartaglino, A.I. Volokitin, E. Tosatti, On the nature of surface roughness with application to contact mechanics, sealing, rubber friction and adhesion. J. Phys.: Condens. Matter **17**(1), R1–R62 (2005)
85. H.O. Peitgen, D. Saupe, Y. Fisher, M. McGuire, R.F. Voss, M.F. Barnsley, R.L. Devaney, B.B. Mandelbrot, *The Science of Fractal Images*, 1st edn. (Springer, New York, 1988)
86. R.F. Voss, Random fractal forgeries, in *Fundamental Algorithms for Computer Graphics*, ed. by R.A. Earnshaw (Springer, Heidelberg, 1985), pp. 805–835
87. G. Anciaux, Simulation multi-échelles des solides par une approche couplée dynamique moléculaire/éléments finis. De la modélisation á la simulation haute performance. Ph.D. thesis, University of Bordeaux (INRIA, CEA), France, July 2007
88. J. Fish, M.A. Nuggehally, M.S. Shephard, C.R. Picu, S. Badia, M.L. Parks, M. Gunzburger, Concurrent AtC coupling based on a blend of the continuum stress and the atomistic force. Comput. Methods Appl. Mech. Eng. **196**(4548), 4548–4560 (2007)
89. K. Fackeldey, R. Krause, Multiscale coupling in function spaceweak coupling between molecular dynamics and continuum mechanics. Int. J. Numer. Meth. Eng. **79**(12), 15171535 (2009)
90. K. Fackeldey, The Weak Coupling Method for Coupling Continuum Mechanics with Molecular Dynamics. Ph.D. thesis, Bonn, February 2009
91. S.B. Ramisetti, G. Anciaux, J.F. Molinari, A concurrent atomistic and continuum coupling method with applications to thermo-mechanical problems. Submitted, 2013